Fluidic beam steering in parasitically coupled patch antenna arrays

ARTICLE *in* ELECTRONICS LETTERS · JULY 2015

Impact Factor: 1.07 · DOI: 10.1049/el.2015.1908

Tonmoy Bhattacharjee
University of Wisconsin–Madison

Fluidic beam steering in parasitically coupled patch antenna arrays

T. Bhattacharjee✉, H. Jiang and N. Behdad

A technique for designing a parasitic patch antenna array whose beam can be steered dynamically using a fluidic tuning mechanism is presented. Using this technique, a three-element patch antenna array operating at 5 GHz is designed and fabricated using 3D printing. Two oil-filled channels are placed in the substrate of the antenna along the radiating edges of the patches and filled with movable metal cylinders and glass balls. The parasitic elements are mutually coupled to the centre element in the *H*-plane. As the train of metal cylinders and glass balls are moved from the left or right with respect to the centre-driven patch element, the beam is steered towards the opposite direction. The proposed parasitic patch array is able to steer the beam ±22.5° with maintained impedance matching.

Introduction: In a switched parasitic antenna, the direction of the radiation pattern can be controlled by electronically changing the characteristics of the nearby parasitic elements close to the driven element [1]. Electronically steerable parasitic array radiators (ESPARs) are closely related to switched parasitic antennas [2–5]. In ESPARs, passive elements are excited through mutual coupling between adjacent elements, which are loaded with tunable reactive loads. Varying the reactive loads of each parasitic element changes the apparent magnitude and phase of the excitation of each element, which results in changing the direction of the beam towards a desired direction. ESPARs can provide a continuous change of the beam direction by using electronically tunable elements. The vast majority of the ESPARs reported in the literature use electronic components, such as solid-state or MEMS varactors [2–5]. Recently, an electronically steerable microstrip patch radiator has been presented in which varactors are loaded between the centre-driven element and the parasitic elements to control the mutual coupling [4]. Varactors are also loaded across the non-radiating edges of the parasitic elements to maintain resonance at the operation frequency and the aperture-coupled feeding technique is also used. This design exhibits only a ±15° continuous scanning range. This example sufficiently illustrates the nature of the work found in the literature related to ESPARs. However, electronically tunable beam steerable antennas suffer from nonlinearities under moderate to high peak-power excitation levels. These nonlinearities can result in intermodulation distortion and RF-induced changes of the antenna's radiation parameters. This limits the use of these tuning techniques mainly to the receiving systems or low-power transceivers.

In this Letter, we present a new technique for designing a parasitic patch array whose beam direction can be steered using a fluidic tuning technique. Such fluidic tuning techniques have recently been demonstrated to be far superior to electronic tuning techniques in terms of linearity of the response of the structure when subjected to moderately high-power levels (tens of watts) [6]. A prototype of the proposed beam-steerable antenna is designed, fabricated and experimentally characterised. The fabricated prototype is composed of a main patch antenna element that is coupled to two adjacent parasitic patches and can provide a beam steering in the ± 22.5° range.

Design procedure: Fig. 1 shows the topology of the proposed antenna. Two 2 mm diameter channels, filled with mineral oil ($\varepsilon_r \approx 2.15$), are located under the radiating edges of the centre and the parasitic patches. The centres of both channels are 3 mm apart from the radiating edges of the centre element. A train of metal cylinders and glass balls are placed inside both channels as shown in Fig. 1*b*. The glass balls are used to maintain uniform spacing between the 10 mm-long and 3 mm-long metal cylinders. When $x_{offset} = 0$ mm, the beam points to the boresight [$+z$ direction, Fig. 1*b*]. The beam is then steered depending on the direction of the movement of the cylinder and ball trains. For example, if the trains move towards the left of the $x_{offset} = 0$ marker ($-x$ direction), the beam is steered towards the opposite direction, i.e. $+x$ direction and vice versa (see Fig. 1). The appropriate placement of the trains along the channels causes the beam to be steered at a specific direction. When x_{offset} (corresponding to channel 1) is 7.9 mm, the beam is steered at 7° off the broadside towards the $+x$ direction. As the beam is steered, the frequency response of the antenna is also affected. However, for all steering angles, the antenna maintains its impedance matching. The placement of the trains in both channels that causes the beam to steer at various angles is summarised in Table 1. Extensive studies have been undertaken to understand the effects of mutual coupling, impedance, and current response in mutually coupled and reactance loaded parasitic array radiators [4–7, 8], and therefore details are not repeated here. The simulations for this antenna were performed using CST Microwave Studio. The placement of the channels, the lengths of the metal cylinders, the appropriate placement of the trains inside the channels, and the dimensions of the centre and parasitic patch elements have been optimised to achieve the desired beam steering angles shown in Table 1.

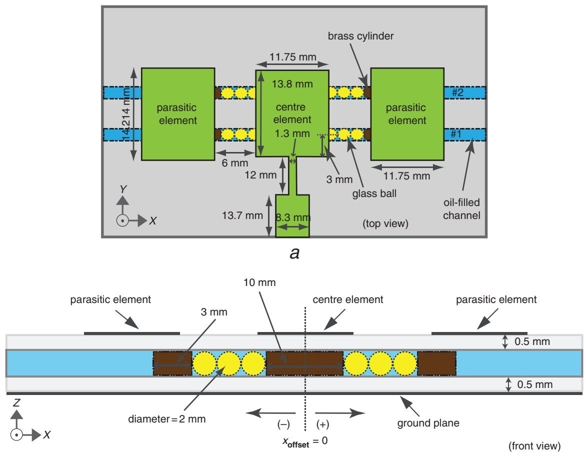

b

Fig. 1 *Layout of mutually coupled proposed parasitic patch array*

a Top view (of the patch array)
b Front view (of the patch array)

Table 1: Summary of beam steering angles at 5.04 GHz (centre frequency of simulated frequency band, 4.88–5.20 GHz) and total efficiency at 5.04 and 5.35 GHz (centre frequency of measured frequency band, 5.30–5.40 GHz)

States	Channel 1 x_{offset} (mm)	Channel 2 x_{offset} (mm)	Scan angle (deg)	Total efficiency	
				Sim. (%)	Meas. (%)
1	0	0	0	58.29	51.50
2	7.9	0	7	59.25	'not meas.'
3	8.9	4.9	15	60.52	59.87
4	8.9	8.9	20	55.97	67.75

Fabrication and measurement results: The substrate of the prototype was fabricated using a Dimension Elite 3D printer. The antenna was designed to operate at around 5 GHz. The overall thickness of the substrate was 3.35 mm and was built with Accura 60, a type of photopolymer resin. The substrate has a dielectric constant of 3.2 and a loss tangent of 0.05 [9]. The patches were fabricated with copper tape on the top surface of the substrate. The channels were loaded with blunt needles and sealed off after they were populated with metal cylinders (brass) and glass balls as shown in Fig. 2. The channels were then filled with mineral oil using 10 ml syringes. By pushing the syringes, the metal cylinders and glass balls are moved to the appropriate positions represented in Table 1. The reflection coefficients were measured using an Agilent N5225A PNA for the first, third and fourth states shown in Table 1. The radiation patterns of the antenna were measured using a multi-probe near-field antenna system at the centre frequency, 5.35 GHz, of the measured frequency band (5.3 – 5.4 GHz) for the three states (see Fig. 3). It can be seen from Fig. 3 that there are discrepancies between the measured and simulated reflection coefficient values. These discrepancies can be attributed to several factors, such as inclusion of tolerance in the final design of the substrate to ensure smooth movement of the cylinders and glass balls inside the channels, imperfections arising in the dimensions of the patches, metal cylinders, glass balls and/or matching network and the limited accuracy of the measurement technique used to characterise the dielectric constant and loss tangent values of the Accura 60 substrate (see [10]). The total efficiencies of the antenna corresponding to states 1, 3 and 4 are reported in Table 1. The relatively small total efficiencies are primarily attributed to the high losses of the 3D-printed dielectric substrate. This, however, is not an inherent limitation of the proposed design. Fig. 4 shows the radiation pattern in the *H*-plane of the antenna for the three states summarised in Table 1. A slight deviation of the steering angles from the simulation for states 1 and 3 can be observed from Fig. 4. This can be attributed to the imprecise positioning of the cylinders and glass balls inside the channels. The maximum steering angle achieved from the prototype was 22.5°. Owing to the symmetry along the *yz*-plane, the antenna would give a maximum steering angle of − 22.5° if the cylinder and glass balls were moved towards the +*x* direction, and therefore measurements were not repeated to demonstrate the negative angle.

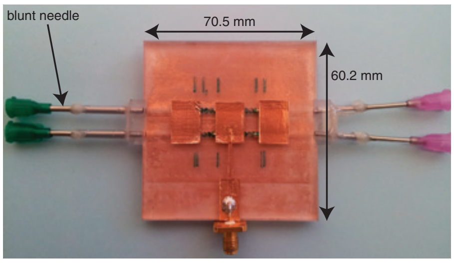

Fig. 2 *Photograph of fabricated prototype*

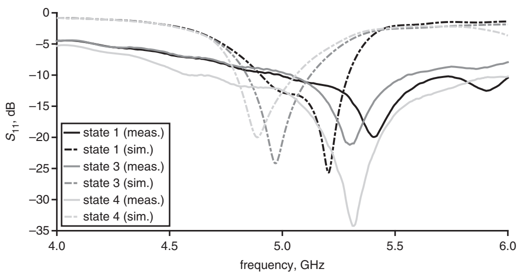

Fig. 3 *Simulated and measured input reflection coefficients of antenna*

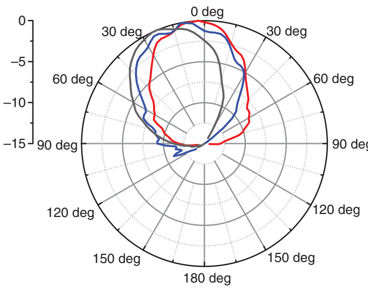

Fig. 4 *Measured normalised H-plane gain patterns of antenna. [Red] state 1 (max gain = 4.47 dBi at 2.8°), [Blue] state 3 (max gain = 5.4 dBi at 11.25°) and [dark grey] state 4 (max gain = 6.28 dBi at 22.5°)*

Conclusion: The design of a parasitic patch array with beam steering capability has been presented and discussed. It was demonstrated that the beam of the antenna can be steered ±22.5° using a fluidic tuning technique. Measurement results show a return loss better than 10 dB and a maximum steering angle of 22.5° when the metal cylinders and glass balls are moved in a specific order in a certain direction. Movement of the cylinders and glass balls in the opposite direction will yield a steering angle of −22.5°. The antenna does not use any type of electronic components and is expected to be useful in systems that need to transmit signals with moderately high peak power levels (tens of watts) while maintaining linearity.

Acknowledgments: This work was supported by the U.S. National Science Foundation under award no. ECCS-1101146. The authors thank A. Momeni and K. Ghaemi (University of Wisconsin Madison) for assistance during measurements.

Submitted: *4 June 2015* E-first: *24 July 2015*
doi: 10.1049/el.2015.1908
One or more of the Figures in this Letter are available in colour online.

T. Bhattacharjee, H. Jiang and N. Behdad (*Department of Electrical and Computer Engineering, University of Wisconsin Madison, Madison, WI 53706, USA*)

✉ E-mail: tbhattacharj@wisc.edu

References

1 Thiel, D.V., and Smith, S.: ‘Switched parasitic antennas for cellular communications’ (Artech House, Norwood, MA, USA, 2002)
2 Harrington, R.: ‘Reactively controlled directive arrays’, *IEEE Trans. Antennas Propag.*, 1978, **AP-26**, (3), pp. 390–395
3 Schlub, R., Lu, J., and Ohira, T.: ‘Seven element ground skirt monopole ESPAR antenna design using a genetic algorithm and the finite element method’, *IEEE Trans. Antennas Propag.*, 2003, **51**, (11), pp. 3033–3039
4 Luther, J.J., Ebadi, S., and Gong, X.: ‘A microstrip patch electronically steerable parasitic patch array radiator (ESPAR) antenna with reactance-tuned coupling and maintained resonance’, *IEEE Trans. Antennas Propag.*, 2012, **60**, (4), pp. 1803–1812
5 Kawakami, H., and Ohira, T.: ‘Electrically steerable passive array radiator (ESPAR) antennas’, *IEEE Antennas Propag. Mag.*, 2005, **47**, (2), pp. 43–49
6 Li, M., and Behdad, N.: ‘Fluidically tunable frequency selective/phase shifting surfaces for high-power microwave applications’, *IEEE Trans. Antennas Propag.*, 2012, **60**, pp. 2748–2759
7 Van Lil, E., and Van De Capelle, A.: ‘Transmission line model for mutual coupling between microstrip antennas’, *IEEE Trans. Antennas Propag.*, 1984, **32**, (8), pp. 816–821
8 Pozar, D.: ‘Input impedance and mutual coupling of rectangular microstrip antennas’, *IEEE Trans. Antennas Propag.*, 1982, **AP-30**, (6), pp. 1191–1196
9 Bhattacharjee, T., Jiang, H., and Behdad, N.: ‘Large-scale fluidic tuning of sub-wavelength periodic structures’, *IEEE Antennas Wirel. Propag. Lett.*, 2015, **14**, pp. 190–193
10 Aguilar, S., Shea, J.D., AL-Joumayly, M.A., *et al.*: ‘Dielectric characterization of PCL-based thermoplastic materials for microwave diagnostic and therapeutic applications’, *IEEE Trans. Biomed. Eng.*, 2012, **59**, pp. 627–633